Available online at www.sciencedirect.com
SCIENCE DIRECT®
International Journal of Heat and Mass Transfer 48 (2005) 3319–3330
International Journal of HEAT and MASS TRANSFER
www.elsevier.com/locate/ijhmt

Measuring and modeling vapor boundary layer growth during transient diffusion heat and moisture transfer in cellulose insulation

Stephen O. Olutimayin, Carey J. Simonson *

Department of Mechanical Engineering, University of Saskatchewan, 57 Campus Drive, Saskatoon, SK, Canada S7N 5A9

Received 1 June 2004; received in revised form 25 February 2005
Available online 21 April 2005

Abstract

In this paper, an experimental test facility that permits continuous measurements of transient heat and moisture transfer in porous media is applied to study the vapor boundary layer in cellulose insulation. The experiment measures the relative humidity, temperature and moisture accumulation within the cellulose specimen with a fully developed flow of air at a controlled temperature and humidity provided above the surface. These experimental results are used to verify a mathematical model, which is used to develop an expression for moisture diffusivity (α_m) that is analogous to thermal diffusivity, and takes into consideration moisture storage. The moisture diffusivity is used to calculate the vapor density in the boundary layer and the size of vapor boundary layer in cellulose insulation. It is found that the moisture storage effect has a very significant effect on the vapor boundary layer and cannot be ignored. For cellulose insulation, the size of the vapor boundary layer may be over predicted by a factor of ten when moisture storage is neglected.

1. Introduction

Most common building insulation materials are porous in nature and many of them are hygroscopic, and thus absorb a significant amount of moisture. The flow of moisture through these materials has a large effect on the heating ventilating and air conditioning (HVAC) system as well as the durability of the building. Over the past decade, a lot of research has been carried out on the effect of moisture transfer and storage in building materials as it affects energy conservation.

Many parts of the world experience large changes in temperature and relative humidity from season to season. But human comfort demands a certain range of temperature and relative humidity in homes and work places throughout the year. An ideal insulation material should be able to minimize the fluctuations in indoor air temperature and relative humidity thereby keeping the sensible and latent loads that need to be met by the HVAC system as small as possible.

Cellulose insulation is an important insulation material that is made almost entirely of re-cycled materials (e.g. newspapers and other paper products). It has a porosity of about 0.95 and provides a high resistance to conduction heat transfer ($K \approx 0.04$ W/(m K) [1–3]. The moisture capacity and resistance are other important parameters because, in addition to temperature, human comfort depends on the indoor relative humidity. The moisture content of the building envelope is also very important and has a large effect on the indoor air

* Corresponding author. Fax: +1 306 966 5427.
E-mail address: carey.simonson@usask.ca (C.J. Simonson).

0017-9310/$ - see front matter © 2005 Published by Elsevier Ltd.
doi:10.1016/j.ijheatmasstransfer.2005.02.024

Nomenclature

C	multiplication constant for the investigation of changes in the sorption isotherm
C_p	specific heat capacity at constant pressure [J/(kg K)]
C_m	moisture storage coefficient defined in Eq. (33)
D_A	binary diffusion coefficient for water vapor in air [m^2/s]
D_{eff}	effective vapor diffusion coefficient [m^2/s]
D_h	hydraulic diameter [m]
h_a	convective heat transfer coefficient [W/(m^2 K)]
h_{fg}	latent heat of vaporization/sorption [J/kg]
h_m	convective mass transfer coefficient [m/s]
K	thermal conductivity [W/(m K)]
K_{eff}	effective thermal conductivity [W/(m K)]
L	overall depth of specimen [m]
$\dot{m}$	rate of phase change [kg/(m^3 s)]
$\dot{m}_a$	mass flow rate of air [kg/s]
Nu	Nusselt number
P	pressure [Pa]
R	specific gas constant [J/(kg K)]
Re	Reynolds number of air flow over the specimen
RH	relative humidity [%]
t	time [s]
T	temperature [°C]
u	mass of moisture adsorbed per kg of dry cellulose [kg/kg]
W	humidity ratio [kg/kg]
x	distance from the top of insulation specimen [m]

Greek symbols

α	thermal diffusivity [m^2/s]
α_m	moisture diffusivity [m^2/s]
$\alpha_{m,eff}$	effective moisture diffusivity [m^2/s] (Eq. (32))
δ_m	vapor boundary layer thickness [m]
Δm	mass of moisture accumulated in the cellulose insulation specimen (g)
ε	volume fraction
ϕ	relative humidity in fraction
ρ	density [kg/m^3]
τ	tortuosity

Subscripts

a	air
f	fluid
g	gas
i	initial
ℓ	adsorbed phase
m	dry cellulose insulation
s	solid
v	vapor
vsat	saturated vapor property
∞	ambient property

quality. Several studies have shown that high moisture contents in indoor air and building materials increase the risk of "sick building syndrome" [4]. Recent studies show that as the indoor relative humidity increases, the indoor air quality becomes more unacceptable [5].

Research has shown that hygroscopic building materials can moderate indoor humidity conditions [6–8]. Simonson et al. [7,8] discovered that moisture transfer between indoor air and hygroscopic structures significantly reduces the peak indoor humidity, which can lead to an improvement in the quality of the indoor air as perceived by the occupants. However, the depth of moisture penetration has not been analyzed in detail and this affects the moisture buffering capacity, which is important to quantify the amount of hygroscopic material that is needed to improve indoor humidity, comfort and air quality conditions [9]. Mendes et al. [10] investigated the effects of moisture on sensible and latent conduction loads by incorporating a heat and mass transfer model into the building energy simulation program DOE-2.1E. Mendes et al. [10] discovered that models that ignore moisture may overestimate conduction peak loads by up to 210% and underestimate the yearly integrated heat flux by up to 59% which could lead to over sizing of HVAC equipment (especially in dry climates) and underestimating the energy consumption (primarily in humid climates).

From a design point of view it would be very desirable to have a simpler expression to predict the size of the vapor boundary layer and the vapor density and moisture content within a porous medium. This would allow HVAC designers to include moisture storage in their design. It would also allow the drying industry to estimate the drying time for different materials more accurately. Transient heat transfer design charts (e.g. Heisler Charts), which take into account the thermal storage capacity, exist and allow for the calculation of temperatures in the boundary layer and the size of the thermal boundary [2]. However the convectional way of trying to estimate similar variables in the vapor boundary layer does not include the moisture storage effect. This paper is aimed at developing a new para-

meter (moisture diffusivity, α_m), which takes into account the moisture storage, to calculate the vapor density in the boundary layer and the size of vapor boundary layer in a hygroscopic material like cellulose insulation.

The experimental work is focused on measuring the moisture accumulation, temperature and relative humidity distribution in a specimen of cellulose insulation subject to a step change in the temperature and relative humidity at the upper boundary. These results are used to validate a numerical model that calculates the heat and moisture transfer in the medium. The analytical model is used to develop an expression for moisture diffusivity (α_m), and α_m is used with an analytical solution to calculate the vapor density and vapor boundary layer thickness in the cellulose insulation specimen.

2. Experiment

The purpose of the experiment is to measure continuously the moisture accumulation, temperature and relative humidity distribution in a cellulose insulation specimen. These measurements will quantify the conditions in the thermal and moisture boundary layers and demonstrate the growth of the boundary layers with time.

A schematic of the apparatus is shown in Fig. 1. The apparatus is designed to create a well-controlled transient, one-dimensional heat and moisture boundary layers within a porous medium. In this paper, a sample of cellulose insulation is packed with a density of 50 kg/m^3 inside a 760 mm × 280 mm × 300 mm container made of Lexan. Other materials can be investigated with appropriate sized containers. An array of T-type thermocouples and capacitance type humidity sensors are arranged in the material to get the temperature and relative humidity distribution in the material as shown in Fig. 1. The humidity sensors were calibrated using a chilled mirror as a transfer standard and have a post calibration bias uncertainty of ±1% RH while the thermocouple wires were calibrated with a temperature simulator and have a post calibration bias uncertainty of ±0.1 °C.

The moisture accumulation is measured via two means; first with load sensors, which support the container holding the cellulose specimen and the second with humidity sensors in the air stream above the insulation. The container is resting on four load sensors in such a way that any change in mass during the experiment is the mass of moisture adsorbed or desorbed from the insulation. The load sensors were calibrated with calibration weights and have a bias uncertainty of ±2 g, which corresponds to ±2% at the end of an 8-h test. The second method of measuring the transient change in moisture content is to integrate with time the difference between the humidity ratio of the air entering and leaving the test section:

$$\Delta m = \int_0^t \dot{m}_a (W_{inlet} - W_{outlet})\, dt. \quad (1)$$

The latter method has a higher uncertainty, mainly due to the uncertainty in the relative humidity measurement, but provides a useful comparison.

The test facility includes a variable speed vacuum pump, which provides a fully developed airflow at the desired temperature and relative humidity over the top of the specimen. The temperature and relative humidity of the supply air is controlled within ±0.1 °C and ±2% RH respectively. The air speed is chosen such that the flow is laminar and the process of transport through the material is pure diffusion i.e., there is no airflow through the insulation specimen so as to prevent convection or any other mode of transport. Temperature sensors located through out the medium verified this. A 38 mm tapered orifice plate is embedded in the supply line to measure the flow rate of the air. The air temperature and pressure difference across the orifice plate are

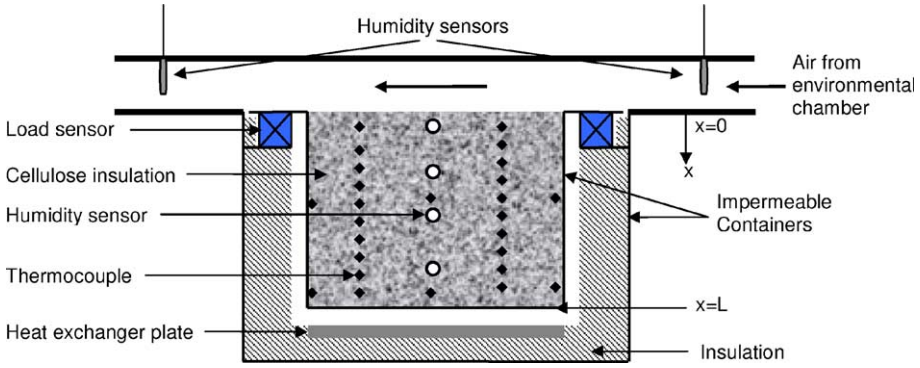

Fig. 1. Schematic of the experimental test section showing the cellulose insulation bed free floating on load sensors with temperature and RH sensors embedded in the material.

measured; thereby making it possible to calculate the mass flow rate of the air according to ISO 5176-1 [11]. The mass flow rate is needed to calculate the moisture accumulation using Eq. (1) and the Reynolds number of the airflow. The uncertainty of the mass flow rate is ±4%.

All the sensors were calibrated before and after the test and there was good agreement between the pre- and post-test calibration. The variations between the pre and post-test calibrations were within the accuracy of the instruments themselves. All the sensors are connected to a data acquisition system that takes continuous measurements in real time.

The test procedure is to allow the cellulose insulation to come to equilibrium with the air in the laboratory (typically 21 °C and 10% RH), which is the initial condition of the test. For the isothermal test, air at temperature of 21 °C and relative humidity of 70% is passed over the cellulose insulation, while for the non-isothermal test, air at temperature of 38 °C and relative humidity of 70% is passed over the cellulose insulation. The isothermal test runs for 8 h and the test is performed three times. The maximum variation in temperature and relative humidity between the three sets of tests are ±0.2 °C and ±1%RH respectively indicating excellent repeatability. Only the average results of the three tests will be presented in this paper. The non-isothermal test runs for 6 h and the results shown are for a single test.

The impermeable Lexan container ensures the one-dimensional moisture transport, while the insulation around the Lexan container ensures the one-dimensional heat transfer. Many type T-thermocouples are placed in the insulation along and across the flow direction. At any depth in the material, the maximum temperature difference along and across the flow direction is 0.2 °C. This shows that the heat transfer is one-dimensional and there is no airflow through the material.

3. Theoretical model

Cellulose insulation is a porous material that is made of irregularly shaped particles; hence it is extremely difficult to analytically define the boundary between each particle and the surrounding fluid. As a result, it is impractical to solve the transport equation continuously for the solid and fluid phase separately because the boundary cannot be defined. The local volume averaging technique, which averages the transport equations and the properties of the solid and fluid phase over a small volume called the representative elementary volume, avoids the problem of analytically defining the boundary between the phases [12]. This technique will be applied in this paper.

Local volume averaging of the energy equation requires that the medium be in local thermal equilibrium. This implies that the point-by-point difference between the temperature of the solid and fluid phase is much smaller compared to the temperature difference across the elementary volume. The medium should also satisfy a length scale such that the particle diameter is very small compared to the length across the elementary volume, while the length across the elementary volume is also very small compared to the overall depth of the material. These criteria are satisfied for the problem investigated in this paper [13].

The following assumptions are made in the development of the model: (1) heat and moisture transfer through the cellulose insulation are one-dimensional; (2) the transport processes within the cellulose insulation are only heat and water vapor diffusion; (3) air and water vapor in the gaseous state behave as ideal gases; (4) the three phases (solid, liquid and gases) are in thermal and moisture equilibrium; (5) the only heat source in the medium is the heat of phase change due to adsorption/desorption of water vapor on cellulose particles, hence there is no chemical reaction; (6) the porous medium properties for cellulose insulation are homogeneous and isotropic; (7) the heat of adsorption is assumed constant; and (8) the solid phase of cellulose insulation medium is assumed to be paper only, i.e. there is no binding agent.

The resulting conservation equations for mass and energy are the averaged transport equations over the elementary volume.

The continuity for the adsorbed phase is,

$$\frac{\partial \varepsilon_\ell}{\partial t} + \frac{\dot{m}}{\rho_\ell} = 0. \tag{2}$$

The gas diffusion of water vapor is,

$$\frac{\partial(\varepsilon_g \rho_v)}{\partial t} - \dot{m} = \frac{\partial}{\partial x}\left(D_{\text{eff}} \frac{\partial \rho_v}{\partial x}\right). \tag{3}$$

The energy transport equation is,

$$\rho C_p \frac{\partial T}{\partial t} + \dot{m} h_{fg} = \frac{\partial}{\partial x}\left(K_{\text{eff}} \frac{\partial T}{\partial x}\right). \tag{4}$$

The rate of phase change is,

$$\dot{m} = -\frac{\partial u}{\partial t}\rho_m, \tag{5}$$

where u is the moisture content (kg/kg) of the insulation. The value of the moisture content at any relative humidity is obtained from the sorption isotherm curve. The experiment to generate the sorption isotherm was performed according to ISO 12571 [14] using salt solutions to generate the relative humidity [15]. The adsorption isotherm curve is shown in Fig. 2, which consists of eight experimental points and a curve fit to obtain a continuous relationship that will be used in the numerical model. Fig. 2 also shows a ±10% change in the curve fit for the sorption isotherm, which is representative of

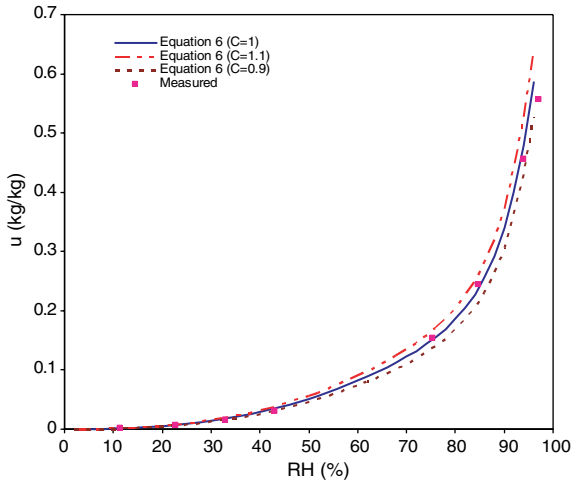

Fig. 2. Sorption isotherm for cellulose insulation showing the measured data, the curve fit and 10% changes in curve fit used in the sensitivity study.

the uncertainty in the measured data and curve fit. These changes will be used in the study to check the sensitivity of moisture content on the vapor density in the numerical model. The equation for the curve fit, which is used in the model to obtain the moisture content is,

$$u = \left(\frac{a + b\phi + c\phi^2 + d\phi^3 + e\phi^4}{3.0 + f\phi + g\phi^2 + i\phi^3 + j\phi^4}\right)C, \tag{6}$$

where $a = -0.00007549$, $b = 0.03947$, $c = 0.5952$, $d = -1.168$, $e = 0.5338$, $f = 6.555$, $g = 23.145$, $i = 17.109$, and $j = -3.522$ and ϕ is the relative humidity as a fraction. Eq. (6) fits the measured data with $R^2 = 0.997$.

The closure equations in the model are as follows.

The volume constraint is,

$$\varepsilon_s + \varepsilon_\ell + \varepsilon_g = 1. \tag{7}$$

The thermodynamic relationships are,

$$\phi = \frac{p_v}{P_{vsat}}, \tag{8}$$

$$P_v = \rho_v R_v T, \tag{9}$$

$$P_g = P_a + P_v, \tag{10}$$

$$P_a = \rho_a R_a T \tag{11}$$

and

$$\rho_g = \rho_a + \rho_v. \tag{12}$$

The changes in material properties due to moisture adsorption are given by the following equations,

$$D_{eff} = \frac{\varepsilon_g D_A}{\tau}, \tag{13}$$

$$\rho = \varepsilon_s \rho_s + \varepsilon_\ell \rho_\ell + \varepsilon_g \rho_g, \tag{14}$$

$$C_p = \frac{\varepsilon_s (\rho C_p)_s + \varepsilon_\ell (\rho C_p)_\ell + \varepsilon_g ((\rho C_p)_a + (\rho C_p)_v)}{\rho} \tag{15}$$

and

$$K_{eff} = \varepsilon_s K_s + \varepsilon_\ell K_\ell + \frac{\varepsilon_g (\rho_a K_a + \rho_v K_v)}{\rho_a + \rho_v}. \tag{16}$$

The boundary conditions for the problem are:

convection @ $x = 0$

$$h_a (T|_{x=0} - T_\infty) = K_{eff} \left.\frac{\partial T}{\partial x}\right|_{x=0}, \tag{17}$$

adiabatic @ $x = L$

$$\left.\frac{\partial T}{\partial x}\right|_{x=L} = 0, \tag{18}$$

convection @ $x = 0$

$$h_m (\rho_v|_{x=0} - \rho_{v,\infty}) = D_{eff} \left.\frac{\partial \rho_v}{\partial x}\right|_{x=0} \tag{19}$$

and impermeable @ $x = L$

$$\left.\frac{\partial \rho_v}{\partial x}\right|_{x=L} = 0, \tag{20}$$

where

$$h_a = \frac{k_a Nu}{D_h} \tag{21}$$

and

$$h_m = \frac{h_a}{\rho_a C_{p_a}}. \tag{22}$$

The Reynolds number for the airflow above the specimen is 1900, giving a Nusselt number of 4.86 [2]. The resulting convective heat and moisture transfer coefficients are 3.4 W/(m^2 K) and 0.0028 m/s.

The initial conditions are constant temperature and relative humidity throughout the insulation specimen, and the initial moisture content is obtained from the sorption curve. The properties of dry cellulose insulation bed used in the experiment and numerical simulation are; $\rho = 50$ [kg/m^3], $K_{eff} = 0.041$ [W/(m K)], $D_{eff} = 1.3 \times 10^{-5}$ [m^2/s] [3], $\tau = 1.9$, $h_{fg} = 2.75 \times 10^6$ [J/kg] [16], $\epsilon_g = 0.947$, and $C_p = 1400$ [J/(kg K)].

3.1. Numerical solution

The coupled partial differential equations are discretized using the finite difference method with second order accuracy for the spatial nodes and the implicit scheme for the time derivative. The central scheme was used for the spatial derivate of the central nodes while the backward or forward scheme is used for the nodes at the boundary. The under relaxed, Gauss-Seidel iteration

method is used to provide a stable solution. The solution is considered to have converged, when for any time step, the change in any dependent property ($T, \rho_v, \varepsilon_\ell, \varepsilon_g$) is less than 10^{-6}.

After initializing all variables and properties, the liquid volume fraction is first calculated from the adsorbed continuity Eq. (2). The temperature and vapor density are then calculated from the energy and vapor transport Eqs. (4) and (3) respectively. The gas volume fraction is calculated from the volume constraint Eq. (7) and the new phase change rate is calculated using Eq. (5). The material properties are then updated from the current dependent variables and the process is repeated until the convergence criteria are satisfied.

A grid mesh of 1 mm (300 grid points) and a time step of 10 s were used in the simulation. Sensitivity studies were carried out on the grid size and time step to check for stability of the numerical solution. A mesh size of 0.1 mm with a time step of 1 s and a mesh size of 0.01 mm with a time step of 1 s were used. The maximum change in relative humidity and temperature are less than 0.15% RH and 0.1 °C respectively for a mesh size of 0.01 mm and time step of 1 s, compared to a 1 mm mesh and 10 s time step, but the run time increased by over 500%. This shows that the solution is stable and increasing the number of nodes and decreasing the time step has a small effect on the numerical results.

4. Experimental data and numerical validation

Two sets of experiments were performed to measure the growth of the thermal and moisture boundary layers and the moisture accumulation within the cellulose insulation. The measured moisture accumulation, temperature and relative humidity distribution in the cellulose insulation are also used to validate the numerical simulation. To verify the numerical model, experimentally determined boundary and initial conditions were used in the numerical simulation so as to obtain a direct comparison between the experiment and numerical simulation.

4.1. Isothermal test

In the first test, the cellulose specimen was initially at equilibrium with air at 21 °C and 11% relative humidity before a laminar air flow (Re = 1900) at 21 °C and 70% relative humidity was passed over the insulation. Fig. 3 shows the measured and simulated relative humidity in the medium for the 8 h test. The results were taken at four spatial points, the last point being 240 mm from the top. There is no significant moisture penetration below this point during the test time. The maximum and average differences between experimental data and

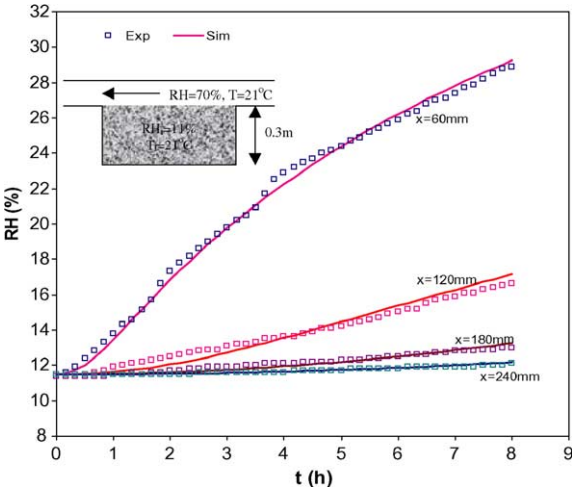

Fig. 3. Experimental and simulated results of relative humidity within the cellulose specimen for the isothermal test.

numerical simulation for the relative humidity in the medium are within 0.4%RH and 0.2%RH respectively. This agreement is excellent and well within the 1% RH experimental uncertainty.

The measured and simulated temperatures clearly show the thermal boundary layer in Fig. 4. The maximum difference between experimental data and numerical simulation is 0.5 °C while the average variation is 0.2 °C. Even though the material and the air passing over it are at the same initial temperature of 21 °C, the temperature in the cellulose bed rose by 6 °C at 60 mm within the first 2 h, which is due to the heat of phase change. After 2 h, the temperature of the insulation at x = 60 mm begins to decrease slightly due to the diffusion of heat into the insulation and convection heat

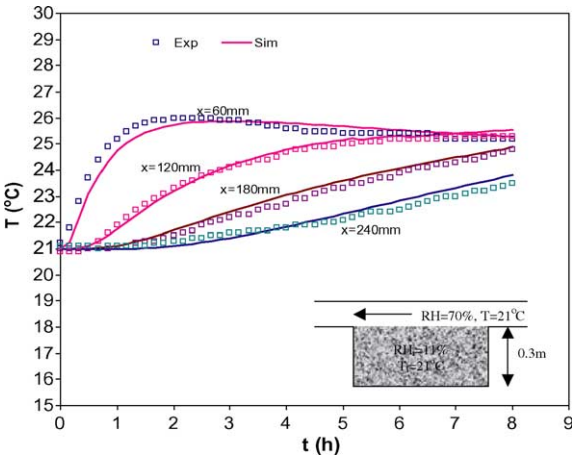

Fig. 4. Experimental and simulated results of temperature distribution within the cellulose specimen for isothermal test.

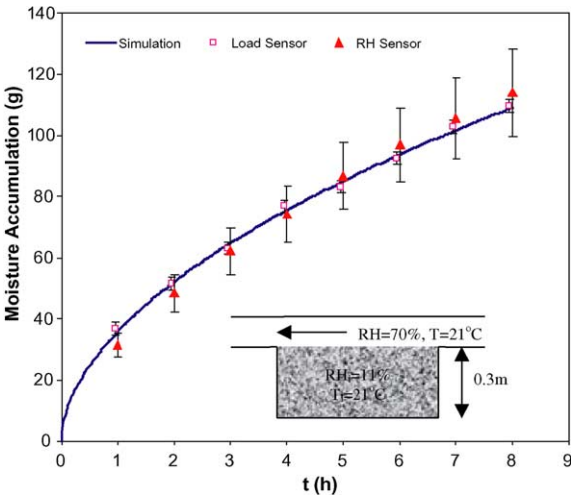

Fig. 5. Experimental and simulated results of moisture accumulation within the cellulose specimen for the isothermal test. The error bars represent the 95% uncertainty bounds for the measured data.

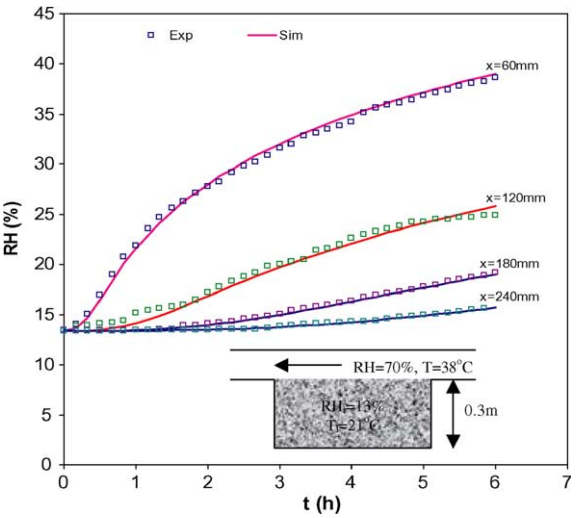

Fig. 6. Experimental and simulated results of relative humidity within the cellulose specimen for the test with a temperature gradient.

transfer to the air above the insulation. The thermal boundary layer grows faster than the vapor boundary layer as can be seen in Figs. 3 and 4. The thermal boundary layer penetrates beyond 240 mm after 2 h, while the water vapor boundary layer requires the full 8 h of the test to reach a depth of 240 mm.

Fig. 5 presents a comparison of the moisture accumulation calculated with the numerical model with that measured using load sensors and the relative humidity sensors in the air stream. All moisture accumulation data follow the same trend with time. The rate of moisture accumulation decreases with time and is consistent with boundary layer growth theory. The moisture accumulation measured using the load sensors shows a better agreement with the simulated results than the data measured with the relative humidity sensors. The maximum difference between the measured and simulated moisture accumulation is less than 3 g for the load sensors and 6 g for the relative humidity sensors. Even though the differences between the simulated data and the measured data using the relative humidity sensors are higher than the difference between the simulated and measured data from the load sensors, the results are well within the uncertainty bounds as shown in Fig. 5.

4.2. Test with a temperature gradient

Figs. 6–8 show the result for relative humidity, temperature and moisture accumulation in the cellulose specimen during a test with a higher air temperature. The initial conditions are nearly the same (21 °C and 13% RH) as in the isothermal test, but the air flowing above the insulation is at 38 °C and 70% RH. In the

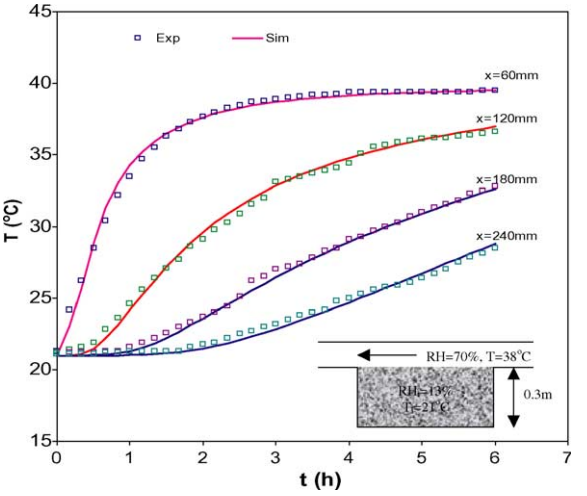

Fig. 7. Experimental and simulated results of temperature distribution within the cellulose specimen for the test with a temperature gradient.

non-isothermal test, there is increase in moisture penetration and accumulation compared to the isothermal test, which is caused by an increase in the vapor pressure difference between the material and the air. The moisture accumulation after 6 h for the isothermal test is 93 g, while the moisture accumulation for the test with a temperature gradient is 173 g showing an increase of 86%.

As in the isothermal test, the moisture boundary layer grows significantly slower than the thermal boundary layer. After 6 h, the temperature distribution is nearly linear with depth, indicating that the

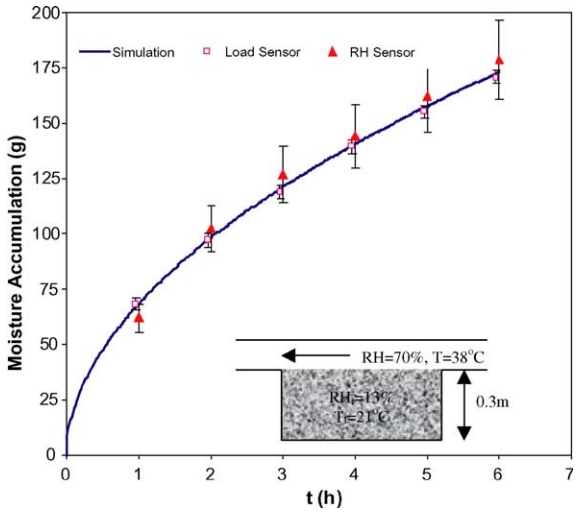

Fig. 8. Experimental and simulated results of moisture accumulation in the cellulose specimen for the test with a temperature gradient.

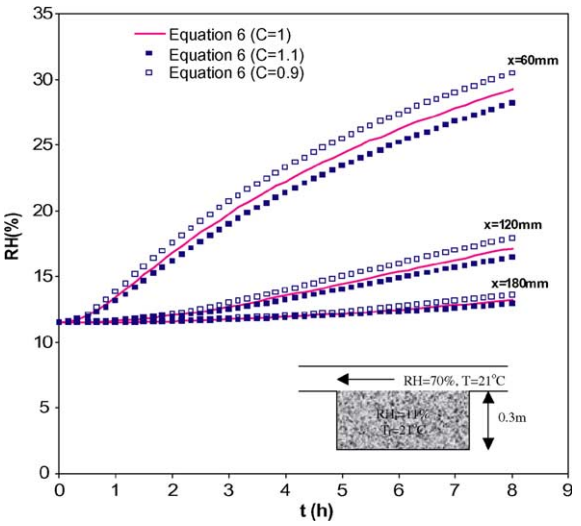

Fig. 9. Sensitivity study on the effect of changing the adsorption isotherm defined in Eq. (6) and Fig. 2 by 10% in the numerical simulation for the isothermal test conditions.

temperatures have nearly reached the steady state values that would exist if the temperature at $x = L$ was fixed at 21 °C. On the other hand, the relative humidity values are far from a linear profile with depth and thus are still developing. The maximum and average differences between the experimental and numerical data for the relative humidity in the bed are 0.5%RH and 0.2%RH respectively. The thermal boundary layer growth shows the same type of agreement as in the isothermal test where the maximum and average differences between experimental data and numerical simulation are within 0.5 °C and 0.2 °C respectively. Measurement of the moisture accumulation using the load sensors and relative humidity sensors show maximum differences of ±4 g and ±7 g respectively compared to the simulated data.

4.3. Sensitivity studies

Sensitivity studies also help verify that the model gives realistic results. The sensitivity of the numerical results to changes in the adsorption isotherm, thermal conductivity, convective heat and moisture transfer coefficients, heat of phase change and binary diffusion coefficient were determined. Increasing the heat of phase change, thermal conductivity, and convective heat coefficient by 10% resulted in an increase in temperature of less than 1%. Increasing the moisture convective coefficient by 10% results in an increase in relative humidity of less than 0.5%.

However, changing the sorption isotherm by 10%, as shown in Fig. 2, had the greatest impact on the moisture boundary layer and these results are presented in Fig. 9. Increasing the adsorption isotherm by 10% ($C = 1.1$ in Eq. (6) and Fig. 2) results in a reduction of 4% in relative humidity, while a reduction of 10% in the adsorption isotherm ($C = 0.9$) increases the relative humidity by 4%. These show that the sorption curve is very important. The results also make physical sense because an increase in adsorption isotherm means that more of the vapor will be adsorbed and there is less to diffuse through the medium and therefore increasing the sorption isotherm results in a decrease in the relative humidity. The sensitivity studies further prove that the results from the numerical model are reliable.

5. Moisture property analogous to thermal diffusivity for calculating vapor boundary layer properties

Significant research has been done on thermal boundary layers resulting in analytical and graphical solutions for transient conduction heat transfer in materials of common geometries [2]. The energy equation for which there are known solutions is,

$$\frac{\partial T}{\partial t} = \alpha \frac{\partial^2 T}{\partial x^2}, \tag{23}$$

and the solutions depend on the boundary conditions. The solution for the case with a surface convection boundary condition for a semi-infinite medium is chosen because it is similar to the experiment presented in this paper. This solution is [2],

$$\frac{T - T_i}{T_\infty - T_i} = \operatorname{erf}c\left(\frac{x}{2\sqrt{\alpha t}}\right) - \left[\exp\left(\frac{h_a x}{k} + \frac{h_a^2 \alpha t}{k^2}\right)\right] \times \left[\operatorname{erf}c\left(\frac{x}{2\sqrt{\alpha t}} + \frac{h_a\sqrt{\alpha t}}{k}\right)\right]. \tag{24}$$

Table 1
Summary of previous and new approach to the thermal moisture property analogy for solving transient moisture transfer

Thermal property	Analogous moisture property (previous)	Analogous moisture property (new)
h_a	h_m	h_m
k	D_{eff}	D_{eff}
$\alpha = \frac{k}{\rho c_p}$	D_{eff}	$\alpha_{m,eff} = \frac{D_{eff}}{C_m}$

With this solution, the temperature at any point in the boundary layer or the size of the thermal boundary layer can be determined from the thermal properties (k, h and α). In order to apply this solution and other thermal solutions for mass transfer problems, it has been common to replace the thermal properties with equivalent moisture properties as shown in Table 1.

Table 1 shows that, in the previous method, the diffusion coefficient (D_{eff}) replaces both the thermal conductivity (k) and the thermal diffusivity (α). The size of the thermal boundary layer depends mostly on thermal diffusivity, which takes into account thermal storage. Ghazi Wakili et al. [17] developed a simple method to measure this thermal diffusivity in an insulation material by measuring the heat flux across the medium. The fact that the diffusion coefficient is typically used as the equivalent moisture property for thermal diffusivity implies that moisture storage is negligible. As shown previously, moisture storage is very important for cellulose insulation (and other hygroscopic materials) and must be included when solving transient moisture transfer. Therefore a new moisture property is needed that is equivalent to thermal diffusivity and includes moisture storage. This property is moisture diffusivity (α_m), as shown in Table 1, and its expression will be developed from the governing equations in the next section.

5.1. Moisture diffusivity (α_m)

The approach here is to write the moisture transfer equation in the same form as the energy equation for which there are known solutions (Eq. (23)) and thereby develop an expression for moisture diffusivity that will be analogous to thermal diffusivity. This new expression for α_m can then be used in place of α in the analytical solution for a given set of boundary condition to determine the vapor density in the boundary layer or the thickness of the boundary layer.

The water vapor transport equation is,

$$\frac{\partial(\varepsilon_g \rho_v)}{\partial t} - \dot{m} = \frac{\partial}{\partial x}\left(D_{eff}\frac{\partial \rho_v}{\partial x}\right). \tag{25}$$

This equation can be written in the same form as Eq. (23) if the phase change rate ($\dot{m}$) can be related to the vapor density.

The expression for phase change,

$$\dot{m} = -\frac{\partial u}{\partial t}\rho_m, \tag{26}$$

is transformed through the following relationships,

$$\frac{\partial u}{\partial t} = \frac{\partial u}{\partial \rho_v}\frac{\partial \rho_v}{\partial t}, \tag{27}$$

and from thermodynamic relationship

$$\rho_v = \frac{\phi P_{vsat}}{R_v T}, \tag{28}$$

to give the phase change rate as a function of the vapor density as follow:

$$\dot{m} = -\frac{\rho_m R_v T}{P_{vsat}}\frac{\partial u}{\partial \phi}\frac{\partial \rho_v}{\partial t}. \tag{29}$$

Substituting Eq. (29) into the water vapor transport Eq. (25) yields,

$$\left(\varepsilon_g + \frac{\rho_m R_v T}{P_{vsat}}\frac{\partial u}{\partial \phi}\right)\frac{\partial \rho_v}{\partial t} = D_{eff}\frac{\partial^2 \rho_v}{\partial \rho_v^2}. \tag{30}$$

The vapor transport equation written in form of Eq. (23) is:

$$\frac{\partial \rho_v}{\partial t} = \alpha_{m,eff}\frac{\partial^2 \rho_v}{\partial \rho_v^2}, \tag{31}$$

where effective moisture diffusivity for a porous media ($\alpha_{m,eff}$) is,

$$\alpha_{m,eff} = \frac{D_{eff}}{C_m}, \tag{32}$$

and

$$C_m = \left(\varepsilon_g + \frac{\rho_m R_v T}{P_{vsat}}\frac{\partial u}{\partial \phi}\right). \tag{33}$$

The term $\frac{\partial u}{\partial \phi}$ is the slope of the sorption curve.

The analytical solution to Eq. (31) for a semi-infinite porous medium with convective boundary conditions can be obtained from Eq. (24) by substituting α with $\alpha_{m,eff}$, k with D_{eff} and h_a with h_m. The solution then becomes:

$$\frac{\rho_v - \rho_{v,i}}{\rho_\infty - \rho_{v,i}} = \operatorname{erfc}\left(\frac{x}{2\sqrt{\alpha_{m,eff}t}}\right) - \left[\exp\left(\frac{h_m x}{D_{eff}} + \frac{h_m^2 \alpha_{m,eff} t}{D_{eff}^2}\right)\right] \times \left[\operatorname{erfc}\left(\frac{x}{2\sqrt{\alpha_{m,eff}t}} + \frac{h_m\sqrt{\alpha_{m,eff}t}}{D_{eff}}\right)\right]. \tag{34}$$

5.2. Verification of α_m

In this section, the measured and simulated vapor boundary layer thickness and vapor densities within the boundary layer in cellulose insulation will be used to verify the expression developed for moisture diffusivity. The situation considered is the isothermal test where

air at a temperature of 21 °C and a relative humidity of 70% is passed over the cellulose insulation specimen, which is initially at temperature of 21 °C and relative humidity of 11%.

The vapor boundary layer thickness (δ_m) is defined as the position in the porous medium where,

$$\frac{\rho_{v,\delta_m} - \rho_{v,i}}{\rho_\infty - \rho_{v,i}} = 0.01. \quad (35)$$

Fig. 10 shows very close agreement between the analytical and simulated values of δ_m for $h_{fg} = 0$ and $\alpha_{m,eff}$ as defined in Eq. (32) (i.e., including moisture storage). On the other hand, δ_m determined from the analytical solution using the previous analogous property (i.e. neglecting moisture storage) is significantly greater than the simulated values. The vapor boundary layer shown in Fig. 10 is for a 0.3m thick cellulose insulation bed. The results obtained from the analytical solution show that if the moisture storage were neglected, the vapor boundary layer would have penetrated out of the cellulose bed after ten minutes; whereas, the simulation indicates that it would take 12 h for the boundary layer to penetrate through the insulation. Excluding the moisture storage term overestimates the vapor boundary layer as much as ten times.

Since heat and moisture transfer are coupled in the experiment, but the analytical solution is for decoupled heat and moisture transfer, the analytical and experimental results cannot be directly compared. However, the importance of the coupling between heat and mass transfer can be seen in Fig. 10 because the moisture boundary layer thickness (δ_m) for coupled heat and moisture transfer ($h_{fg} \neq 0$) obtained from numerical simulation and experimental data is also included. With the inclusion of the coupling, the vapor boundary layer is twice as thick as when there is no coupling. This increase in δ_m due to the coupling of heat and mass transfer is expected because the heat released during the adsorption of water vapor on the cellulose particles increases the temperature in the medium thereby increasing the vapor pressure. As the vapor pressure increases, the vapor penetration also increases as shown previously in the experimental results with a temperature gradient. It should be noted that including the coupling is not as critical as including the moisture storage term; however, further work is necessary to develop an expression to include the coupling of the energy and vapor transport equations.

The moisture diffusivity (α_m) is further verified by calculating the vapor density in the boundary layer using Eq. (34) and comparing the results with simulated values. These results are for the isothermal test condition (and $h_{fg} = 0$) and are presented in Fig. 11. The maximum difference between the simulated results and the results using Eq. (34) is 2%. These differences are mostly due to approximations used when computing the complementary error function in Eq. (34).

5.3. Sensitivity studies

According to Eqs. (31) and (34), the vapor boundary layer thickness at a given time depends on h_m, D_{eff} and C_m. The purpose of this section is to investigate how sensitive δ_m is to these parameters (Fig. 12). Fig. 12 shows that a 10% increase in C_m reduces δ_m by 6% whereas a 10% reduction in C_m increases δ_m by 6%. An increase in C_m, increases the moisture storage

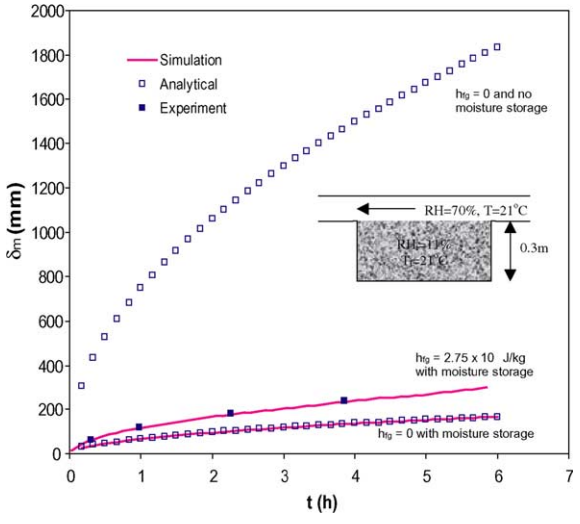

Fig. 10. Vapor boundary layer thickness in cellulose insulation specimen with and without moisture storage, and also for coupled ($h_{fg} = 2.75 \times 10^6$ J/kg) and decoupled ($h_{fg} = 0$) heat and moisture transport equations.

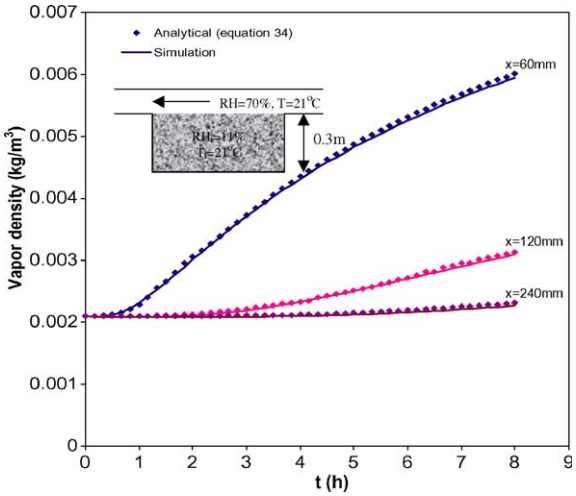

Fig. 11. Simulated and analytical results using Eq. (34) of the vapor density in the boundary layer for an isothermal test condition with $h_{fg} = 0$.

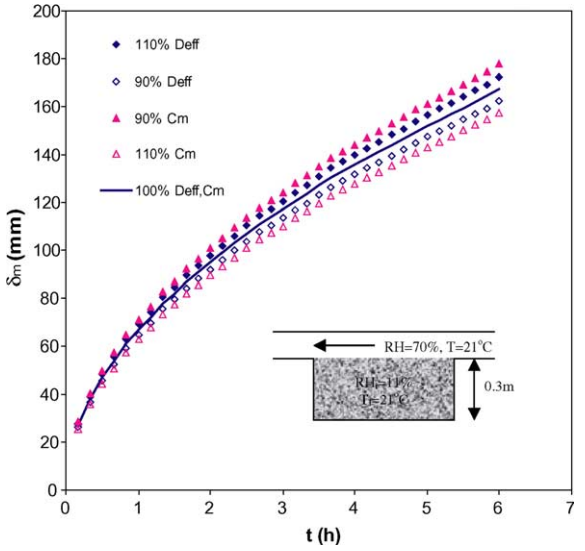

Fig. 12. Sensitive study of changes by 10% in C_m and D_{eff} on the vapor boundary layer thickness for isothermal test conditions.

capacity or the water vapor adsorbed, thereby reducing the water vapor penetration in the medium. A 10% change in D_{eff}, changes δ_m by 3%. However a 10% change in h_m only results in 1% change in δ_m and is not presented in Fig. 12.

The results from the sensitivity studies show that C_m (which is very dependent on the slope of the sorption curve) is the most sensitive parameter in obtaining the vapor boundary layer thickness. This result confirms the earlier sensitivity study, which showed that the sorption curve is the most sensitive property in obtaining the relative humidity (or vapor density) in the boundary layer.

6. Conclusions

In this paper, one dimensional and transient, heat and moisture transfer by means of diffusion in a porous cellulose insulation bed was investigated numerically and experimentally. The theoretical model was used to develop an expression for a moisture property (α_m) analogous to thermal diffusivity that includes moisture storage. The moisture diffusivity (α_m) allows the heat transfer solutions in the literature to be applied to moisture transfer problems to determine, for example the vapor density in the boundary layer or the vapor boundary layer thickness. The following conclusion can be made.

1. A new experimental method to measure continuously and accurately the moisture accumulation, thermal and vapor boundary layer growth in porous media was developed and applied to hygroscopic cellulose insulation.
2. A new moisture property (moisture diffusivity) analogous to thermal diffusivity, which takes into account moisture storage, was developed to calculate the vapor boundary layer thickness in cellulose insulation.
3. The heat of phase change causes a significant rise in temperature in the cellulose bed even when the air and medium have the same initial temperature.
4. Results from the sensitivity studies show that the moisture transfer and vapor boundary layer thickness in cellulose insulation are most sensitive to the sorption curve.
5. The accuracy of the vapor density in the boundary layer and the vapor boundary layer thickness calculated from analytical expressions or numerical models depend on the inclusion of the moisture storage term. Neglecting moisture storage over predicts the boundary layer thickness by an order of magnitude for cellulose insulation.

Acknowledgement

Financial support from the following sources in acknowledged: Natural Sciences and Engineering Research Council of Canada (NSERC), Canada Foundation for Innovation (CFI) and the University of Saskatchewan (College of Graduate Studies and Research New Faculty Graduate Student Support Program and the Department of Mechanical Engineering Devolved Scholarship Fund).

References

[1] ASHRAE, Fundamentals Handbook 2001, Atlanta.
[2] F.P. Incropera, D.P. Dewitt, Fundamentals of Heat and Mass Transfer, John Wiley & Sons, New York, 2001.
[3] C.J. Simonson, M. Salonvaara, T. Ojanen, Moderating indoor conditions with hygroscopic building materials and outdoor ventilation, ASHRAE Trans. 110 (2) (2004) 804–819.
[4] J. Sundel, What we know, and don't know about Sick Building Syndrome, ASHRAE J. 38 (1996) 51–57.
[5] J. Toftum, P.O. Fanger, Air humidity requirements for human comfort, ASHRAE Trans. 105 (2) (1999) 641–647.
[6] P. Plathner, M. Woloszyn, Interzonal air and moisture transport in a test house: experiment and modeling, Build. Environ. 37 (2) (2002) 189–199.
[7] C.J. Simonson, M. Salonvaara, T. Ojanen, The effect of structures on indoor humidity—possibility to improve comfort and perceived air quality, Indoor Air 12 (2002) 243–245.
[8] C.J. Simonson, M. Salonvaara, T. Ojanen, Heat and mass transfer between indoor air and a permeable and hygroscopic building envelope. Part I: Field measurements, J. Therm. Envel. Build. Sci. 28 (1) (2004) 63–101.

[9] C. Rode, A. Holm, T. Padfield, A review of humidity buffering in the interior spaces, J. Therm. Environ. Build. Sci. 27 (2004) 221–226.
[10] N. Mendes, P.C. Philippi, R. Lamberts, A new mathematical method to solve highly coupled equations of heat and mass transfer in porous media, Int. J. Heat Mass Transfer 45 (2002) 509–518.
[11] ISO, Measurement of fluid flow by means of pressure differential devices, ISO 5176-1, Switzerland, 1991.
[12] M. Kaviany, Principles of Heat Transfer in Porous Media, Springer-Verlag, New York, 1991.
[13] S.O. Olutimayin, Vapor boundary layer growth during transient heat and moisture transfer in cellulose insulation, M.Sc. thesis, University of Saskatchewan, Saskatoon, SK, 2004.
[14] ISO, Building Materials- Determination of hygroscopic sorption curves, ISO 12571, Brussels, 1996.
[15] ASTM, Maintaining constant relative humidity by means of aqueous solutions, ASTM E 104, Philadelphia, 1985.
[16] Y.-X. Tao, R.W. Besant, C.J. Simonson, Measurement of the heat of adsorption for a typical fibrous insulation, ASHRAE Trans. 98 (1992) 495–501.
[17] K. Ghazi Wakili, B. Binder, R. Vonbank, A simple method to determine the specific heat capacity of thermal insulations used in building construction, Energy Build. 35 (2003) 413–415.